

N-Body Simulations of Gas-free Disc Galaxies with SMBH Seed in Binary Systems

R. CHAN¹

¹*Observatório Nacional, Coordenação de Astronomia e Astrofísica, Rua General José Cristino 77, São Cristóvão,
CEP 20921-400, Rio de Janeiro, RJ, Brazil.*

ABSTRACT

We have shown the outcome of N-body simulations of the interactions of two disc galaxies without gas with the same mass. Both disc galaxies have halos of dark matter, central bulges and initial supermassive black hole (SMBH) seeds at their centers. The purpose of this work is to study the mass and dynamical evolution of the initial SMBH seed during a Hubble cosmological time. It is a complementation of our previous paper with different initial orbit conditions and by introducing the SMBH seed in the initial galaxy. The disc of the secondary galaxy has coplanar or polar orientation in relation to the disc of the primary galaxy and their initial orbit are eccentric and prograde. The primary and secondary galaxies have mass and size of Milky Way with an initial SMBH seed. We have found that the merger of the primary and secondary discs can result in a final normal disc or a final warped disc. After the fusion of discs, the final one is thicker and larger than the initial disc. The tidal effects are very important, modifying the evolution of the SMBH in the primary and secondary galaxy differently. The mass of the SMBH of the primary galaxy have increased by a factor ranging from 52 to 64 times the initial seed mass, depending on the experiment. However, the mass of the SMBH of the secondary galaxy have increased by a factor ranging from 6 to 33 times the initial

SMBH seed mass, depending also on the experiment. Most of the accreted particles have come from the bulge and from the halo, depleting their particles. This could explain why the observations show that the SMBH with masses of approximately $10^6 M_\odot$ are found in many bulgeless galaxies. Only a small number of the accreted particles has come from the disc. In some cases of final merging stage of the two galaxies, the final SMBH of the secondary galaxy was ejected out of the galaxy.

Keywords: Simulation, disc galaxy, supermassive black hole, binary galaxies, merger, warped disc galaxies

1. INTRODUCTION

It is well known in the literature that supermassive black holes (SMBH) exist in the majority of the galaxies, within elliptical, disc to even in dwarf galaxies [(Kormendy & Ho 2013), (Moran 2014)].

Several recent works in numerical simulations with SMBH with gas [(Tremmel et al. 2018), (Sanchez et al. 2018), (Curd & Narayan 2018)] show us how complex is the dynamical evolution and mass growing with gas accretion can be.

Moreover, many papers have been published about simulations of binary mergers with BH seeds including complex dissipative processes but not included in the present simulations [(Springel, Di Matteo & Hernquist 2005), (Di Matteo et al. 2008), (Khan 2018), (Gabor et al. 2016), (Callegari et. 2009), (Hopkins et al. 2005), (Hopkins et al. 2006), (Chapon, Mayer & Teyssier 2013), (Mayer et al. 2007)].

Simulations of binary mergers with BH seeds and no dissipative effects, similar to the ones presented in this work are published by several authors [(Li et al. 2017), (Governato, Colpi & Maraschi 1994), (Ebisuzaki, Makino & Okumura 1991), (Makino 1993), (Makino 1996), (Khan et al. 2012), (Rantala et al. 2018), (Makino 1997)].

On the other hand, there are only few works in the literature based on simulations of interaction of gas-free disc galaxies [(Oh et al. 2008), (Dobbs et al. 2010), (Lotz et al. 2010), (Struck et al. 2011)]

(Bois et al. 2011), (Chan & Junqueira 2003), (Chan & Junqueira 2014)] but none has treated the problem of the existence of a SMBH at center of the galaxies.

In a recent paper of Li et al. (2017) it is presented the results of the gas-free interaction of SMBHs in very eccentric galaxy orbits. Besides, there are rare works studying the evolution of such binary galaxy in a long interval of time [(Chan & Junqueira 2001), (Chan & Junqueira 2003), (Chan & Junqueira 2014)], in small eccentricity orbits. This work is a complementation of our previous work (Chan & Junqueira 2014), where, there, the focus was the evolution of the discs, but here we use different initial orbit conditions and with a SMBH seed in the initial galaxy. Thus, differently, we will focus in the SMBH seed evolution in a cosmological time and covering a wider range of orbits of the galaxy binary than in the work of Li et al. (2017).

Thus, the main goal of the present work is to perform numerical N-body simulations to study the time evolution of the mass and dynamics of the initial SMBH seed in the two disc galaxies. We also want to know if the tidal forces affect the evolution of the SMBH.

This paper explores the scenario as follows: first, we assume a disc galaxy with the characteristics of the Milky Way (disc, bulge, halo and SMBH). Second, we let a secondary galaxy with the same characteristics orbit on prograde coplanar or polar disc (orientation in relation to the primary disc galaxy).

The paper is organized as follows: in Section 2 we describe the numerical method used in the simulations. In Section 3 we present the initial conditions. In Section 4 we describe the results of the simulations. Finally, in Section 5 we summarize the results.

2. NUMERICAL METHOD

The N-body simulation code used was GADGET (Springel et al. 2001). A modified version of this basic code was made in order to introduce the SMBH gravitational interaction with the other particle. Here we have used only the N-body integration but without gas.

The units used in all the simulations are $G = 1$, [length] = 4.500 kpc, [mass] = $5.100 \times 10^{10} M_{\odot}$, [time] = 1.993×10^7 years ($H_0 = 100$ km/s/Mpc) and [velocity] = 220.730 km/s. Hereinafter, all the physical quantities will be referred to these units. The Hubble time t_H corresponds to 490 time units.

We assumed in all the simulations the tolerance parameter $\theta = 0.577$. The energy is conserved to better than 6% during the entire evolution with a time step size $\Delta t = 1.000 \times 10^{-3}$ and the softening parameter $\epsilon = 8.000 \times 10^{-4}$.

As mentioned above, we have utilized in this work a modified version of the GADGET code (Springel et al. 2001), in order to mimic the interaction of the galaxy particles with the SMBH particle. We have assumed that the collisions between the galaxy particles and the SMBH particle are inelastic. The collision is in such way that they fuse with the SMBH particle with the total mass as a sum of the two ones.

The Schwarzschild radius of the SMBH is define as

$$R_{bh} = \frac{2M_{bh}}{c^2}, \quad (1)$$

where M_{bh} is the SMBH mass and c is the light velocity.

We also have assumed if a galaxy particle with softening parameter ϵ and it grazes the Schwarzschild radius of the SMBH, following the Equation (2), they are merged with one single SMBH particle (see Figure 1). Thus, the Schwarzschild radius increases because of the additional merged galaxy mass particle with the SMBH.

Definition of the condition when there is a merge between the galaxy and the SMBH particle

$$D \leq R_{bh} + \epsilon, \quad (2)$$

where D is the distance between the centers of the SMBH and the galaxy particle, ϵ is the particle softening parameter and R_{BH} is the Schwarzschild radius of the SMBH.

This is clearly an oversimplified scenario of accretion of galaxy mass onto a SMBH which has, in reality, a much more complex physics involved. At least, with this study, we can know approximately the evolution of the SMBH mass and its dynamical evolution in binary galaxies during a long-time evolution.

In order to determine the number of bulge/halo/disk particles accreted onto the SMBH as a function of time we have saved a snapshot at each time step of 4.9 time units until the Hubble time $t_H = 490$ of both galaxies, primary and secondary. Thus, at the end of each experiment we have 100 saved

Table 1. Disc galaxy model properties

Galaxy	M_d	N_d	R_d	Z_d	R_t	M_b	N_b	M_h	N_h
G_1	0.871	40,000	1.000	0.100	5.000	0.425	19,538	4.916	225,880

M_d is the disc mass, N_d the number of particles of the disc, R_d the disc scale radius, Z_d the disc scale height, R_t the disc truncation radius, M_b the bulge mass, N_b the number of particles in the bulge, M_h the halo mass, N_h the number of halo particles.

snapshot files. Each snapshot file generated by the modified GADGET code has an identification number, position, velocity and mass of each particle. In this way we can identify the bulge/halo/disk galaxy structure that each particle belongs. When a given particle is merged with the SMBH, using the condition (2), we sum the mass of this particle with the previous mass of the SMBH and set zero mass to this particle. Besides, we recalculate the new position and velocity of the SMBH after the inelastic collision and then we let evolve the system again. At the end of each experiment we count how many bulge/halo/disk particles with zero mass that certainly have merged with the SMBH. Thus, we can obtained the time evolution of the bulge/halo/disk accreted onto the SMBH.

3. INITIAL CONDITIONS OF THE SIMULATIONS

We have utilized the self-consistent disc-bulge-halo galaxy model by Kuijken & Dubinski (Kuijken & Dubinski 1995) in the simulations, the same as in our previous paper (see Table 1 and Table 2) (Chan & Junqueira 2014). We have also introduced a SMBH seed at rest and at the center of the mass of the galaxy, in order to study its mass and dynamical evolution.

Our simulations have been utilized fewer particles than other works on gas-free disc galaxies but without an initial SMBH seed. In order to try to answer the questions proposed here, we have run small simulations using the available computer clusters, to have, at least, an initial mass and dynamical study of the SMBH seed.

4. THE RESULTS OF THE SIMULATIONS

We have run several simulations, without the secondary galaxy to check the initial structure of the galaxy model with the initial SMBH seed at rest at its center (see Figures 2-6). For the simulations

Table 2. Continuation of Table 1

Galaxy	m	ϵ	M_{BH}	R_{bh}
G_1	2.1764×10^{-5}	8.0000×10^{-4}	2.1764×10^{-4}	2.3597×10^{-10}

m the mass of each particle, and ϵ is the softening of each particle. M_{bh} the SMBH mass, R_{bh} the SMBH radius,

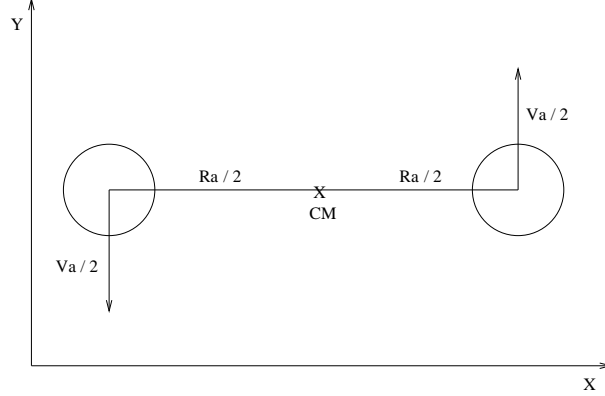


Figure 1. Schematic plot showing the initial positions and velocities of the primary and secondary galaxies. The quantities R_a and V_a are given in the Table 3 and Table 4. CM denotes the center of the mass of the binary.

with the primary and secondary galaxies we have used two clusters: SGI ICE-X and BULL-X BLADE B500, The maximum number of CPU processors have used for both clusters were 32. Each simulation took about 45 days (BULL-X BLADE B500) and 31 days (SGI ICE-X) of CPU time in average.

In Figure 2 we show the contour plot of the primary galaxy at the beginning of the simulation ($t = 0$) and at the Hubble time of the simulation ($t = t_H$). We note that the central density in the plane XY has increased slightly after one Hubble time of simulation, since the contour levels are the same for the two moments of time.

Comparing Figures 3 and 4, we note from the quantity $\langle V_z^2 \rangle^{1/2}$ that the self-heating of the initial disc and the particle halo adds significant source of heating in the disc. The softening can also cause the disc to heat up. Moreover, the total rotation curves V_c and the angular momentum in the Z direction have not changed at the time $t = t_H$ of the simulation. The maximum of the rotation curve $V_c^{max} = 2.5$ occurs at $R_{max} = 2$.

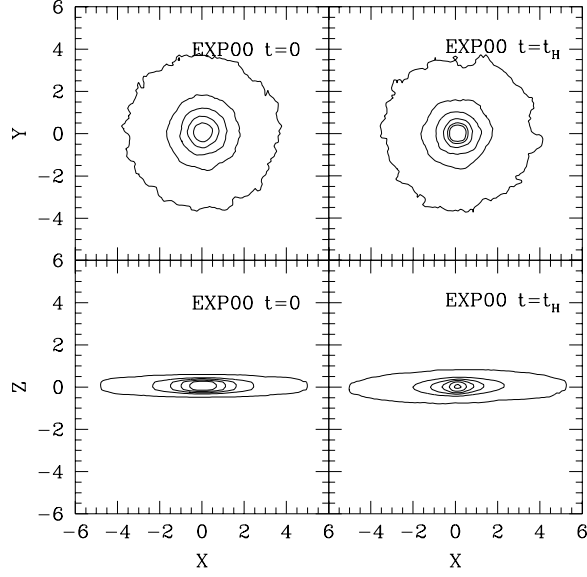


Figure 2. Contour plot of the primary galaxy G_1 at the times $t = 0$ and $t = t_H$). The smoothing was made by averaging the 25 first and second neighbors of each pixel. The density levels in the planes XY and XZ at $t = 0$ are used in contour plots, in the planes XY and XZ at $t = t_H$.

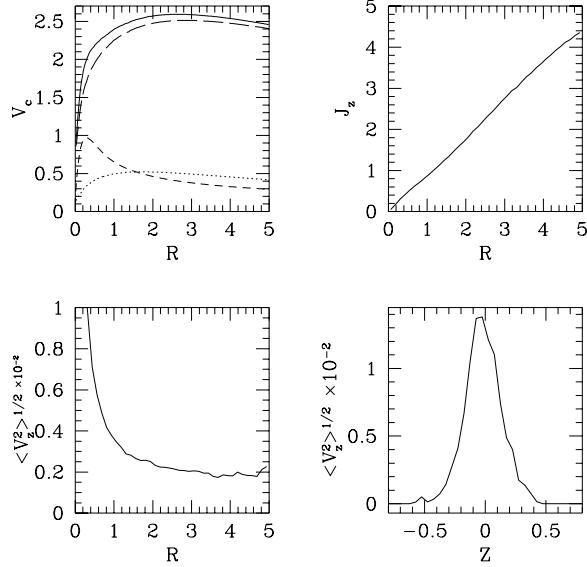


Figure 3. Rotation curve of the galaxy G_1 of the disc V_c , the angular momentum per unit of mass J_z and the velocity dispersion in the z direction $\langle V_z^2 \rangle^{1/2}$ at the time $t = 0$. Hereinafter, the coordinate R is the radius in cylindrical coordinates. The dotted line denotes the disc, the long-dashed line denotes the bulge, the short-dashed line denotes the halo, and the solid line denotes the total rotation curve.

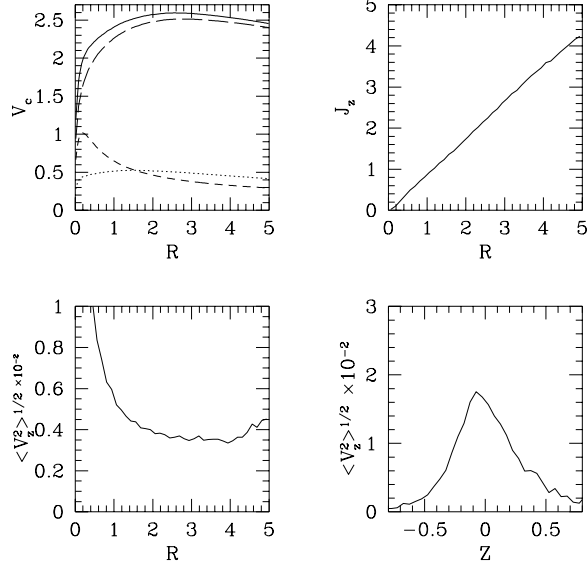


Figure 4. Rotation curve of the galaxy G_1 of the disc V_c , the angular momentum per unit of mass J_z and the velocity dispersion in the z direction $\langle V_z^2 \rangle^{1/2}$ at the time $t = t_H$. The dotted line denotes the disc, the long-dashed line denotes the bulge, the short-dashed line denotes the halo, and the solid line denotes the total rotation curve.

In Figures 5 and 6 we present the temporal evolution of the scale radius R_d and the scale height Z_d . Because of the heating of the disc the first quantity diminishes with the time while the second increases with the time. The linear fitting parameters of these two quantities are presented in the captions of these figures. In the XZ plane the scale height has increased 8% because of the two-body relaxation heating (Figure 6).

Comparing all the results presented in Figures 2-6 with our previous work (Chan & Junqueira 2014) at $t = t_H$ for the same quantities we can show that they are very similar to ours here, except the rotation curve V_c (Figure 4) and the scale height Z_d (Figure 6). In the previous paper we have obtained that the maximum of the rotation curve $V_c^{max} = 1.2$ occurs at $R_{max} = 0.2$ and the scale height Z_d increased only 0.2%. The differences are caused mainly because of the initial SMBH seed.

All the initial conditions of the numerical experiments are presented in Table 3 and Table 4. The orbits of the initial galaxies are eccentric ($e = 0.1, 0.4$ or 0.7) and the orientations of the discs are

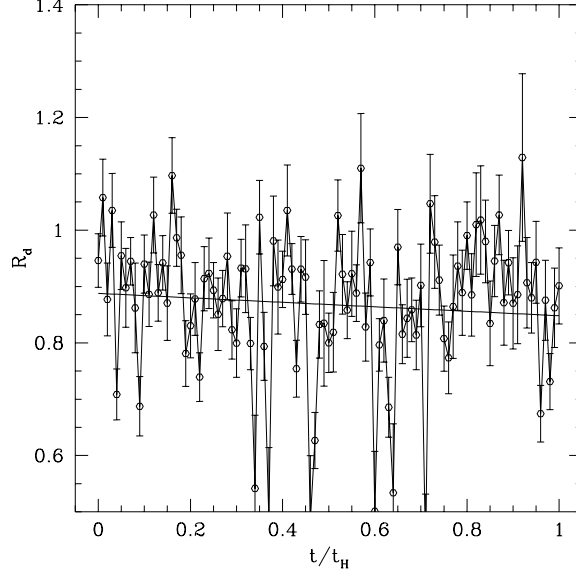


Figure 5. The evolution in time of the scale radius R_d . The projected particle number density on the XY plane was fitted using the sech disc approximation for each instant of time. This approximation was also used in our previous work (Chan & Junqueira 2014). The linear fitting parameters are $R_d = (0.8878 \pm 0.1993 \times 10^{-1})[t/t_H] + (0.8878 \pm 0.1993 \times 10^{-1})$.

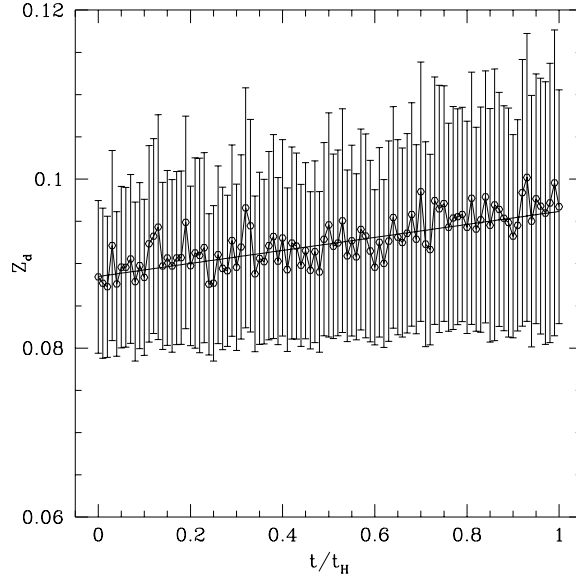


Figure 6. The evolution in time of the scale height Z_d . The projected particle number density on the XZ plane was fitted using the sech disc approximation for each instant of time, as used in our previous work (Chan & Junqueira 2014). The linear fitting parameters are $Z_d = (0.8848 \times 10^{-1} \pm 0.3456 \times 10^{-3})[t/t_H] + (0.7696 \times 10^{-2} \pm 0.6771 \times 10^{-3})$.

Table 3. Primary and secondary galaxy initial conditions

EXP	Θ	R_p	e	R_a	V_a	M_{bh}
00						2.1764×10^{-4}
01	0	12	0.1	14.67	0.8732	2.1764×10^{-4}
02	0	12	0.4	28.00	0.5160	2.1764×10^{-4}
03	0	12	0.7	68.00	0.2341	2.1764×10^{-4}
04	0	15	0.1	18.33	0.7810	2.1764×10^{-4}
05	0	15	0.4	35.00	0.4615	2.1764×10^{-4}
06	0	15	0.7	85.00	0.2094	2.1764×10^{-4}
07	0	20	0.1	24.44	0.6763	2.1764×10^{-4}
08	0	20	0.4	46.67	0.3997	2.1764×10^{-4}
09	0	20	0.7	113.33	0.1814	2.1764×10^{-4}
10	0	23	0.1	28.11	0.6307	2.1764×10^{-4}
11	0	23	0.4	53.67	0.3727	2.1764×10^{-4}
12	0	23	0.7	130.33	0.1691	2.1764×10^{-4}
13	0	25	0.1	30.56	0.6049	2.1764×10^{-4}
14	0	25	0.4	58.33	0.3575	2.1764×10^{-4}
15	0	25	0.7	141.67	0.1622	2.1764×10^{-4}
16	0	30	0.1	36.67	0.5522	2.1764×10^{-4}
17	0	30	0.4	70.00	0.3263	2.1764×10^{-4}
18	0	30	0.7	170.00	0.1481	2.1764×10^{-4}

Θ the angle between the two planes of the discs in units of degree, R_p the pericentric distance, M_1 the primary galaxy mass, e the eccentricity, R_a the apocentric distance, V_a the velocity at the apocentric distance, M_1 the primary galaxy mass, and $M_2 = M_1 = 0.621$ is the secondary mass galaxy. In these experiments the orbits of the particles of both galaxies, primary and secondary galaxy, have clockwise rotations.

coplanar ($\Theta = 0$) or polar ($\Theta = 90$) to each other. The simulations always have begun with the primary and secondary galaxies at the apocentric positions.

Table 4. Continuation of Table 3

EXP	Θ	R_p	e	R_a	V_a	M_{bh}
19	90	12	0.1	14.67	0.8732	2.1764×10^{-4}
20	90	12	0.4	28.00	0.5160	2.1764×10^{-4}
21	90	12	0.7	68.00	0.2341	2.1764×10^{-4}
22	90	15	0.1	18.33	0.7810	2.1764×10^{-4}
23	90	15	0.4	35.00	0.4615	2.1764×10^{-4}
24	90	15	0.7	85.00	0.2094	2.1764×10^{-4}
25	90	20	0.1	24.44	0.6763	2.1764×10^{-4}
26	90	20	0.4	46.67	0.3997	2.1764×10^{-4}
27	90	20	0.7	113.33	0.1814	2.1764×10^{-4}
28	90	23	0.1	28.11	0.6307	2.1764×10^{-4}
29	90	23	0.4	53.67	0.3727	2.1764×10^{-4}
30	90	23	0.7	130.33	0.1691	2.1764×10^{-4}
31	90	25	0.1	30.56	0.6049	2.1764×10^{-4}
32	90	25	0.4	58.33	0.3575	2.1764×10^{-4}
33	90	25	0.7	141.67	0.1622	2.1764×10^{-4}
34	90	30	0.1	36.67	0.5522	2.1764×10^{-4}
35	90	30	0.4	70.00	0.3263	2.1764×10^{-4}
36	90	30	0.7	170.00	0.1481	2.1764×10^{-4}

Θ the angle between the two planes of the discs in units of degree, R_p the pericentric distance, M_1 the primary galaxy mass, e the eccentricity, R_a the apocentric distance, V_a the velocity at the apocentric distance, M_1 the primary galaxy mass, and $M_2 = M_1 = 0.621$ is the secondary mass galaxy. In these experiments the orbits of the particles of both galaxies, primary and secondary galaxy, have clockwise rotations.

We will show only the evolution time of the SMBH of the experiments where the two discs merge or graze each other, where the tidal effects are more prominent during the evolution of the simulation

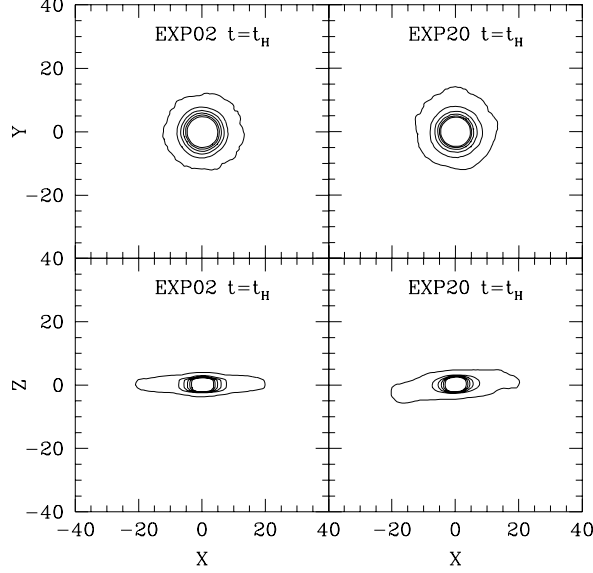


Figure 7. Contour plots of the final merged discs at $t = t_H$ of the experiments EXP02 and EXP20.

(see Table 5-6). The experiments are: EXP02 (Figure 8), EXP06 (Figure 9), EXP20 (Figure 10) and EXP24 (Figure 11).

Comparing the contour plots of the discs at $t = t_H$ shown in Figure 7 for the experiments EXP02 and EXP20 we can note that the merger of the primary and secondary discs can result in a final normal disc (EXP02) or a final warped disc (EXP20). After the fusion of discs, the final one is thicker and larger than the initial discs.

In Figures 8a-11a we show the time evolution of the SMBH mass of the primary and secondary galaxy of the experiments EXP02, EXP06, EXP20 and EXP24. We also present the time evolution of the SMBH mass of the isolated galaxy in the Figures 8a-11a, in order to compare its SMBH mass growth to the SMBH mass growth of the primary and secondary galaxy during the evolution. In the same plots we show the temporal evolution of the distance of the center of mass between the two galaxies. There is an arbitrary scale factor only to adjust the distance within the plot scale of each figure. The purpose of these plots is to know if the distance approach of the primary and secondary galaxies to each other increases the mass growth of the SMBHs.

The Figures 8b-11b and Figures 8c-11c show the time evolution of the number of accreted particles of the primary and secondary galaxy onto the SMBHs, respectively. These plots show how many halo, bulge and disc particles that contribute to the growth of SMBH mass.

Comparing the Figures 8a-11a we can notice the tidal effects in the SMBH mass of the secondary galaxy are more important (see the distance of the center of mass between the two galaxies in the plot). The approach of the galaxies to each other seems not to affect too much the primary galaxy (see Table 5-6).

Comparing the Figures 8b-11b and Figures 8c-11c, respectively, we can note that most of the accreted particles onto the SMBH have come from the bulges and from the halos. Only a small number of the accreted particles onto the SMBH has come from the discs.

In some cases of final merging stage of the two galaxies, the final SMBH of the secondary galaxy is ejected out of the galaxy (see Table 5-6).

From Table 5-6 we can see comparing the final SMBH mass of all the experiments that the mass of the SMBH of the primary galaxy have increased by a factor ranging from 52 to 64 times the initial seed mass, depending on the experiment. However, the mass of the SMBH of the secondary galaxy have increased by a factor ranging from 6 to 33 times in comparison to the initial seed mass, depending on the experiment. Thus, we can conclude that the tidal effects are very important, modifying the evolution of the SMBH in the primary and secondary galaxy differently.

5. CONCLUSIONS

We have shown the results of N-body simulations of the interactions of two gas-free disc galaxies with the same mass. Both disc galaxies have halos of dark matter, central bulges and initial SMBH seeds at their centers.

We have found that the merger of the primary and secondary discs can result in a final normal disc or a final warped disc. After the fusion of discs, the final one is thicker and larger than the initial disc.

The tidal effects are very important, modifying the evolution of the SMBH in the primary and secondary galaxy differently. The mass of the SMBH of the primary galaxy have increased by a

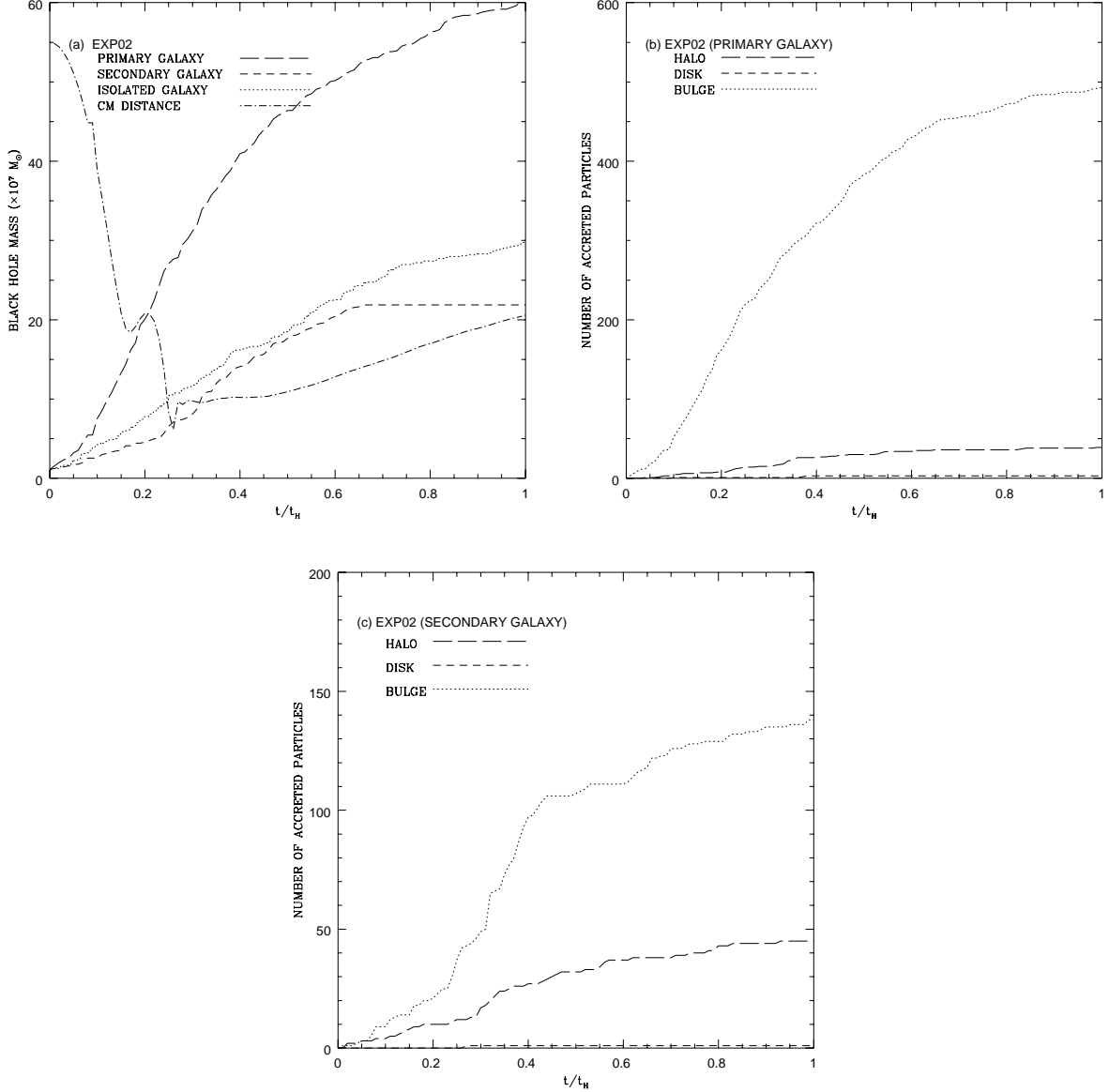


Figure 8. (a) Temporal evolution of the SMBH seed mass of the primary (long-dashed line) and secondary galaxy (short-dashed line) of the experiment EXP02. We also present the time evolution of the SMBH seed mass of the isolated galaxy. In the same plot we show the temporal evolution of the distance of the center of mass of the two galaxies (dot-dashed line). There is an arbitrary scale factor only to adjust the distance within the plot scale. (b) and (c) Time evolution of number of accreted particles of the primary and secondary galaxy onto the SMBH. The long-dashed lines represent the halo particles. The dotted lines represent the bulge particles. The short-dashed lines represent the disk particles.

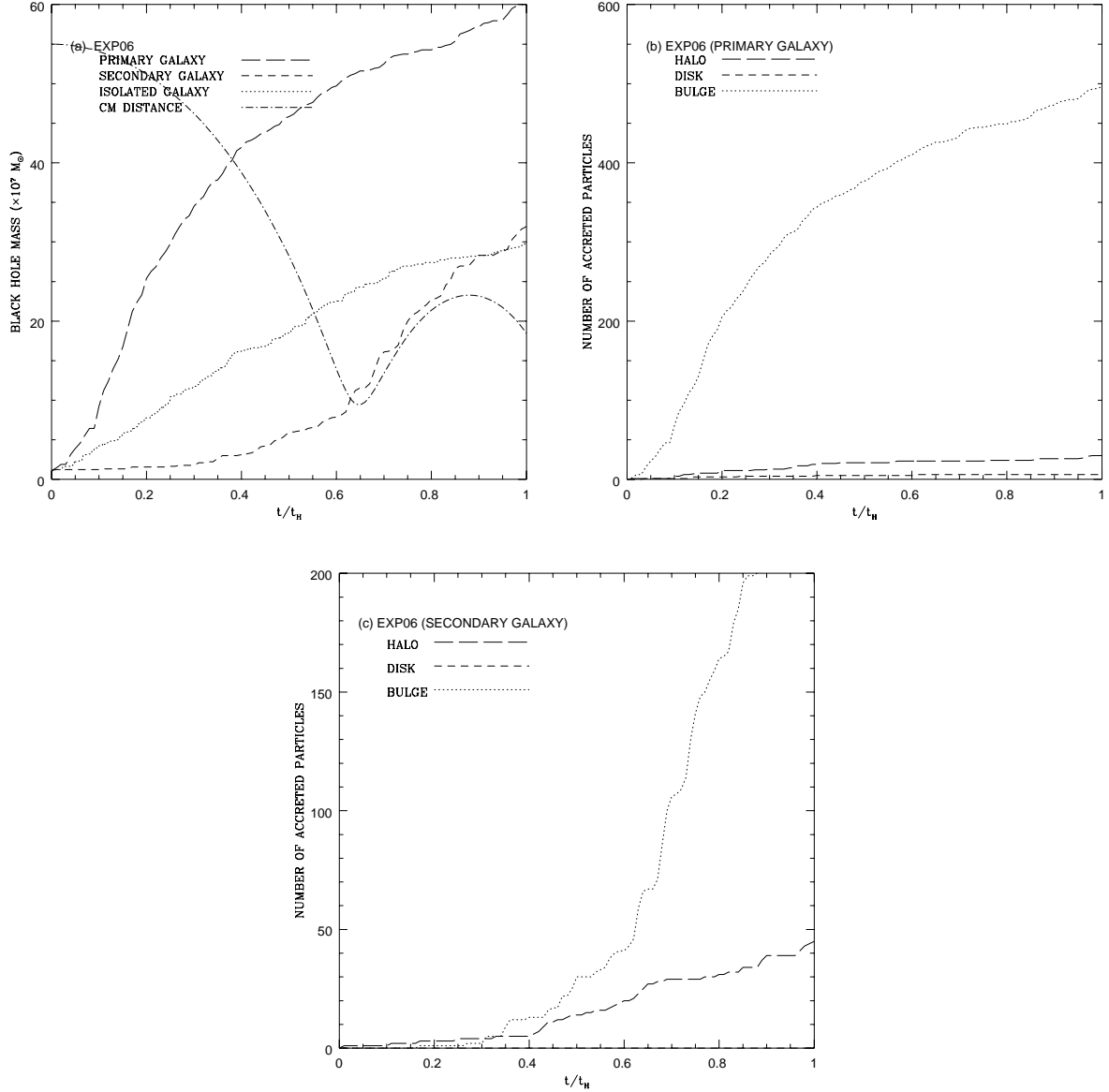


Figure 9. (a) Temporal evolution of the SMBH seed mass of the primary (long-dashed line) and secondary galaxy (short-dashed line) of the experiment EXP06. We also present the time evolution of the SMBH seed mass of the isolated galaxy. In the same plot we show the temporal evolution of the distance of the center of mass of the two galaxies (dot-dashed line). There is an arbitrary scale factor only to adjust the distance within the plot scale. (b) and (c) Time evolution of number of accreted particles of the primary and secondary galaxy onto the SMBH. The long-dashed lines represent the halo particles. The dotted lines represent the bulge particles. The short-dashed lines represent the disk particles.

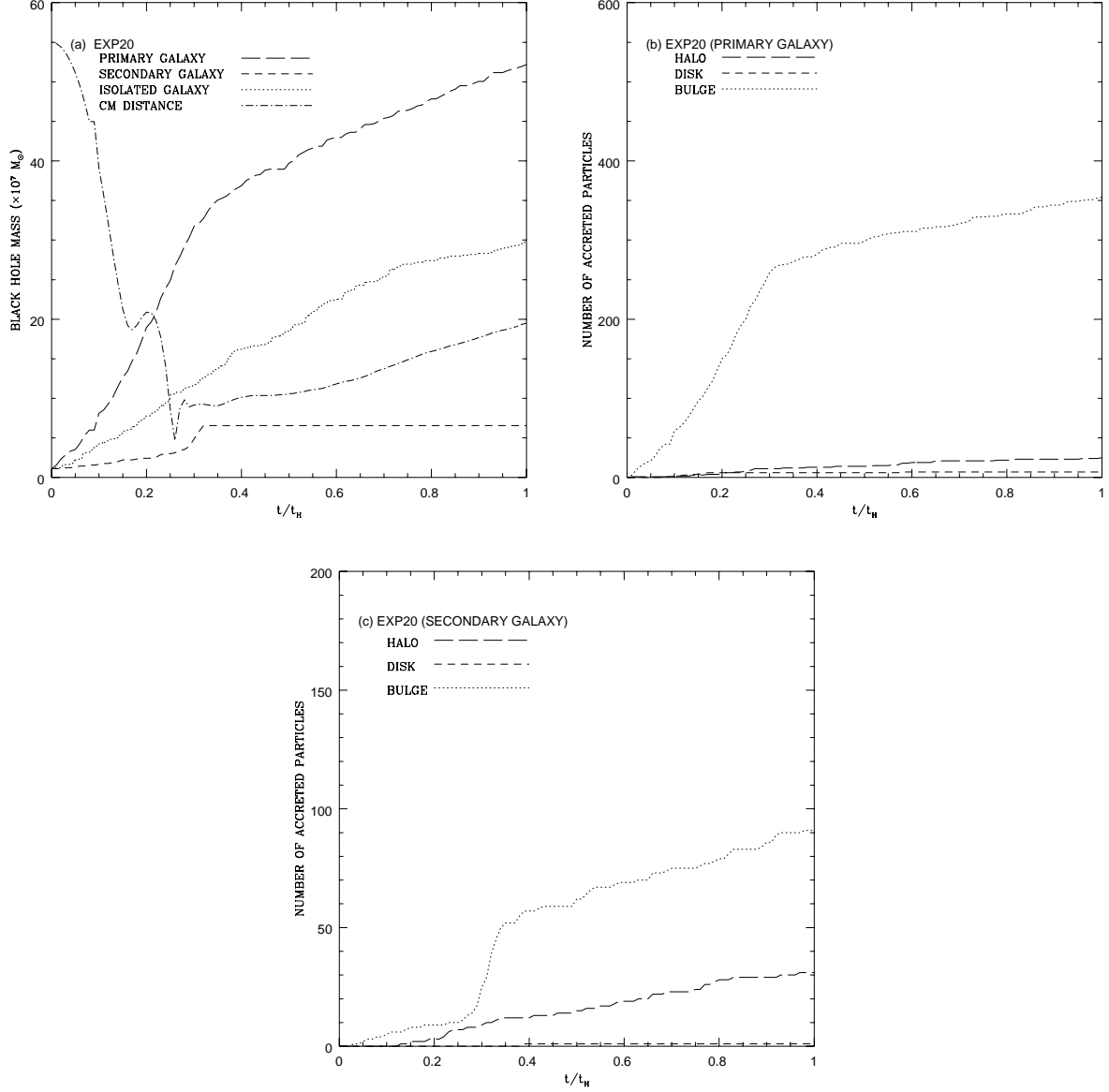


Figure 10. (a) Temporal evolution of the SMBH seed mass of the primary (long-dashed line) and secondary galaxy (short-dashed line) of the experiment EXP20. We also present the time evolution of the SMBH seed mass of the isolated galaxy. In the same plot we show the temporal evolution of the distance of the center of mass of the two galaxies (dot-dashed line). There is an arbitrary scale factor only to adjust the distance within the plot scale. (b) and (c) Time evolution of number of accreted particles of the primary and secondary galaxy onto the SMBH. The long-dashed lines represent the halo particles. The dotted lines represent the bulge particles. The short-dashed lines represent the disk particles.

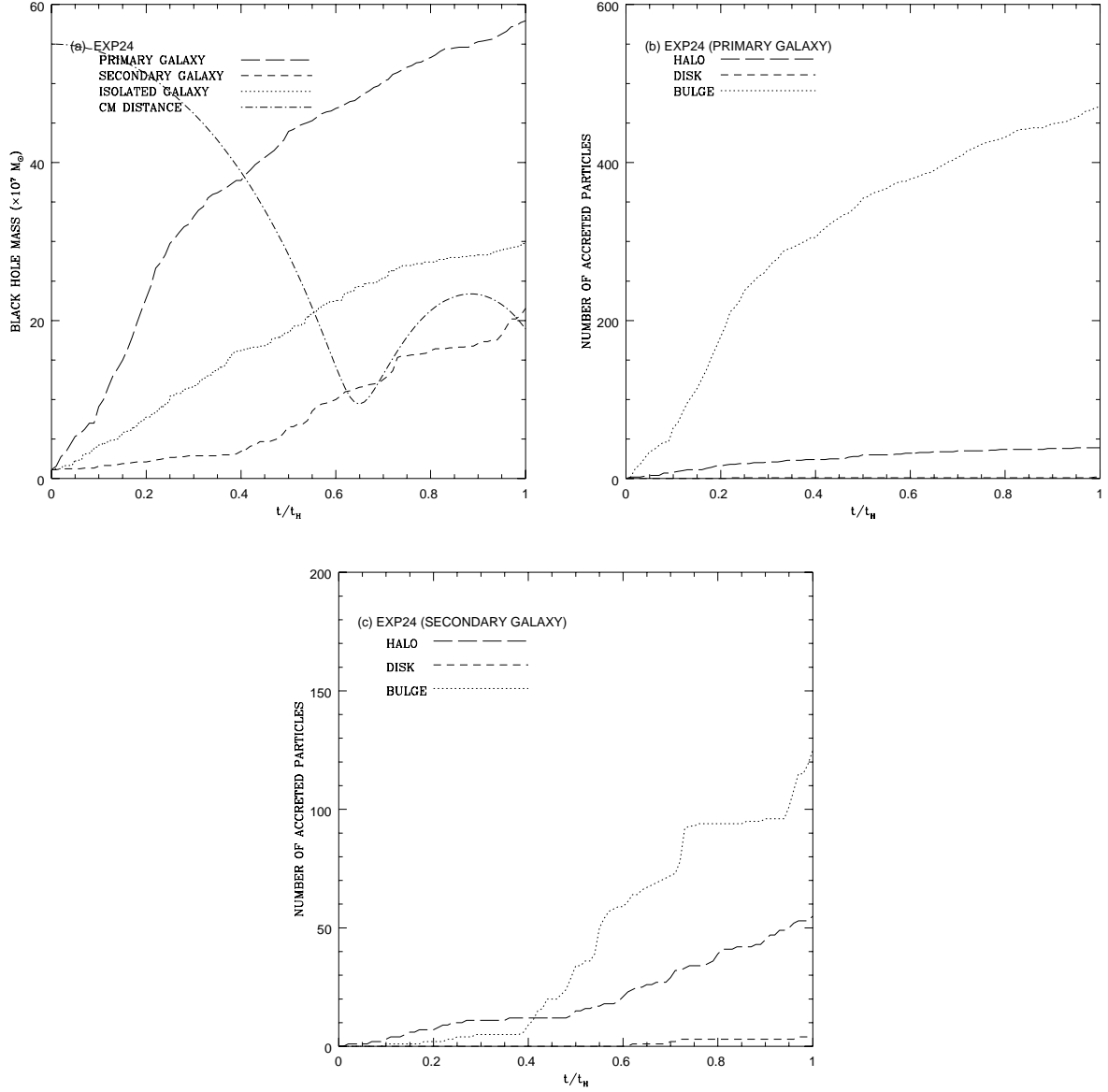


Figure 11. (a) Temporal evolution of the SMBH seed mass of the primary (long-dashed line) and secondary galaxy (short-dashed line) of the experiment EXP24. We also present the time evolution of the SMBH seed mass of the isolated galaxy. In the same plot we show the temporal evolution of the distance of the center of mass of the two galaxies (dot-dashed line). There is an arbitrary scale factor only to adjust the distance within the plot scale. (b) and (c) Time evolution of number of accreted particles of the primary and secondary galaxy onto the SMBH. The long-dashed lines represent the halo particles. The dotted lines represent the bulge particles. The short-dashed lines represent the disk particles

Table 5. Characteristics of galaxy orbits and SMBH mass at t_H

EXP	Disc Interaction	Primary SMBH	Secondary SMBH
01	Merge	58.0533	16.7611*
02	Merge	60.1646	21.8667*
03	Merge	63.4899	23.3100*
04	Merge	52.2800	33.8553
05	Merge	58.4970	14.4299*
06	Graze	60.1646	31.9683
07	Merge	59.1651	29.4152
08	Merge	67.0445	31.9678
09	Distant	57.4974	17.3160
10	Merge	59.4966	30.7468
11	Distant	58.9406	23.8649
12	Distant	62.9391	16.4281
13	Merge	60.7155	31.3022
14	Distant	61.9394	22.9770
15	Distant	61.3836	18.6481
16	Distant	58.7214	27.3059
17	Distant	64.2702	21.3118
18	Distant	60.2718	15.4290

Initial mass of SMBH of the primary and secondary galaxy is 1.1099, Primary SMBH and Secondary SMBH in units of $10^7 M_\odot$, *Graze* means that the two discs touch each other for a while and then separate. *Merge* means that the two discs fuse. *Distant* means the two discs interacts apart each other. The symbol (*) after the mass of the SMBH of some merging experiments means that the SMBH has been ejected out of the binary system during the evolution of the merged binary.

factor ranging from 52 to 64 times the initial seed mass, depending on the experiment. However, the mass of the SMBH of the secondary galaxy have increased by a factor ranging from 6 to 33 times the initial SMBH seed mass, depending also on the experiment.

Table 6. Continuation of Table 5

EXP	Disc Interaction	Primary SMBH	Secondary SMBH
19	Merge	53.6111	26.8622
20	Merge	52.1679	6.5489*
21	Merge	62.0517	16.5387*
22	Merge	53.3919	27.3059
23	Merge	54.1670	13.8750
24	Graze	57.9411	21.5337
25	Merge	54.8352	14.2080
26	Merge	62.0517	21.8667
27	Distant	58.1654	21.2012
28	Merge	58.8284	23.4212
29	Distant	60.4962	24.3091
30	Distant	61.3836	18.8700
31	Merge	61.8273	21.3118
32	Distant	62.3832	21.3118
33	Distant	61.7151	21.7560
34	Distant	61.6029	24.8640
35	Distant	59.3843	21.9779
36	Distant	61.0521	21.2007

Initial mass of SMBH of the primary and secondary galaxy is 1.1099, Primary SMBH and Secondary SMBH in units of $10^7 M_\odot$, *Graze* means that the two discs touch each other for a while and then separate. *Merge* means that the two discs fuse. *Distant* means the two discs interacts apart each other. The symbol (*) after the mass of the SMBH of some merging experiments means that the SMBH has been ejected out of the binary system during the evolution of the merged binary.

Most of the accreted particles have come from the bulges and from the halos, depleting their particles. This could explain why the observations show that the SMBH with masses of approximately

$10^6 M_{\odot}$ are found in many bulgeless galaxies (Kormendy & Ho 2013). However, only a small number of the accreted particles has come from the disc.

In some cases of final merging stage of the two galaxies, the final SMBH of the secondary galaxy was ejected out of the galaxy.

ACKNOWLEDGMENTS

The author acknowledges the the financial support from Conselho Nacional de Desenvolvimento Científico e Tecnológico - Brazil.

The author also thanks the generous amount of CPU time given by CENAPAD/UFC (Centro Nacional de Processamento de Alto Desempenho da UFC) and NACAD/COPPE-UFRJ (Núcleo de Avançado de Computação de Alto Desempenho da COPPE/UFRJ) in Brazil. In addition, this research has been supported by SINAPAD/Brazil.

REFERENCES

- Kormendy, J. & Ho, L.C., 2013, *ARA & A*, 51, 511
- Moran, E.C., Shahinyan, K., Sugarman, H.R.,
Velez, D.O. & Eracleous, M., 2014 *AJ*, 148, 136
- Tremmel, M., Governato, F., Volonteri, M., Quinn,
T. R. & Pontzen, A., 2018, *MNRAS* 475, 4967
- Sanchez, N.N., Bellovary, J.M.,
Holley-Bockelmann, K., Tremmel, M., Brooks,
A. Governato, F., Quinn, T., Volonteri, M.,
Wadsley, J., 2018, *AJ*, 860, 20
- Curd, B. & Narayan, R., 2018, *MNRAS*, sty3134
- Oh, S.H., Kim, W., Lee, H. M. & Kim, J. 2008,
ApJ 683, 94
- Dobbs, C.L., Theis, C., Pringle, J.E. & Bate,
M.R. 2010, *MNRAS* 403, 625
- Lotz, J.M., Jonsson, P., Cox, T.J. & Primack,
J.R. 2010, *MNRAS*, 404, 575
- Struck, C., Dobbs, C.L., & Hwang, J. 2011,
MNRAS, 414, 2498
- Bois, M., Emsellem, E., Bournaud, F., Alatalo,
K., Blitz, L., Bureau, M., Cappellari, M.,
Davies, R.L., Davis, T.A., de Zeeuw, P.T., Duc,
P., Khochfar, S., Krajnovi, D., Kuntschner, H.,
Lablanche, P., McDermid, R.M., Morganti, R.,
Naab, T., Oosterloo, T., Sarzi, M., Scott, N.,
Serra, P., Weijmans, A. & Young, L.M. 2011,
MNRAS, 416, 1654
- Chan, R. & Junqueira, S., 2001, *A & A*, 366, 418
- Chan, R. & Junqueira, S., 2003, *ApJ*, 586, 780
- Chan, R. & Junqueira, S., 2014, *A& A* 567, 17

- Kuijken, K. & Dubinski, J., 1995 MNRAS 277, 1341
- Springel, V., Yoshida, N. & White, S.D.M., 2001, New Astronomy 6, 79
- Li, S., Liu, F.K., Berczik, P. and Spurzen, R., 2017 ApJ, 834, 195
- Mayer, L., Kazantzidis, S, Madau, P., Colpi, M., Quinn, T. and Wadsley, J., 2007 Science 316, 1874
- Hopkins, P.F., Somerville, R.S., Hernquist, L., Cox, T.J., Robertson, B., and Li, Y., 2006 ApJ 652, 864
- Hopkins, P.F., Hernquist, L., Cox, T.J., Di Matteo, T., Martini, P., Robertson, B. and Springel, V., 2005 ApJ 630, 705
- Rantala, A., Johansson, P.H., Naab, T., Thomas, J. and Frigo, M., 2018 ApJ 864, 113
- Khan, F.M., Berentzen, I., Berczik, P., Just, A., Mayer, L., Nitadori, K. and Callegari, S., 2012 ApJ 756, 30
- Callegari, S., Mayer, L., Kazantzidis, S., Colpi, M., Governato, F., Quinn, T. and Wadsley, J., 2009 ApJ, 696, L89
- Chapon, D., Mayer, L. and Teyssier, R., 2013 MNRAS 429, 3114
- Ebisuzaki, T., Makino, J. and Okumura, S.K., 1991, Nature 354, 212
- Makino, J., 1997, ApJ 478, 58
- Makino, J. and Ebisuzaki, T., 1996, ApJ 465, 527
- Makino, J. Fukushima, T., Okumura, S.K. and Ebisuzaki, T., 1993 PASJ 45, 303
- Governato, F., Colpi, M. and Maraschi, L., 1994 MNRAS 271, 317
- Khan, F.M., Capelo, P.R., Mayer, L. and Berczik, P., 2018 ApJ 868, 97
- Gabor, J.M., Capelo, P.R., Volonteri, M., Bournaud, F., Bellovary, J., Governato, F. and Quinn, T., 2016 A&A 592, 62
- Di Matteo, T., Colberg, J., Springel, V., Hernquist, L. and Sijacki, D. 2008 ApJ 676, 33
- Springel, V., Di Matteo, T. and Hernquist, L. 2005 MNRAS 361, 776